Magnetic phase diagram of Ba_{3}CoSb_{2}O_{9} as determined by ultrasound velocity measurements

G. Quirion, M. Lapointe-Major, M. Poirier, J. A. Quilliam, Z. L. Dun, and H. D. Zhou

Phys. Rev. B **92**, 014414 — Published 13 July 2015

DOI: 10.1103/PhysRevB.92.014414

Magnetic phase diagram of $Ba_3CoSb_2O_9$ as determined by ultrasound velocity measurements.

G. Quirion,* M. Lapointe-Major, M. Poirier, and J. A. Quilliam
Département de Physique, Université de Sherbrooke, Sherbrooke, Québec J1K 2R1, Canada

Z. L. Dun and H. D. Zhou
Department of Physics and Astronomy, University of Tennessee, Knoxville, Tennessee, 37996-1200, USA

Using high resolution sound velocity measurements we have obtained a very precise magnetic phase diagram of $Ba_3CoSb_2O_9$ a material that is considered to be an archetype of the spin 1/2 triangular-lattice antiferromagnet. Results obtained for the field parallel to the basal plane (up to 18 T) show three phase transitions, consistent with predictions based on simple 2D isotropic Heisenberg models and previous experimental investigations. The phase diagram obtained for the field perpendicular to the basal plane clearly reveals an easy-plane character of this compound and in particular, our measurements show a single first order phase transition at $H_{c1} = 12.0\ T$ which can be attributed to a spin-flop between an umbrella-type configuration and a coplanar V-type order where spins lie in a plane perpendicular to the *ab*-plane. A low temperatures softening of the lattice within some of the ordered phases is also observed and may be a result of residual spin fluctuations.

PACS numbers: 75.30.Kz, 75.50.Ee, 74.25.Ld

I. INTRODUCTION

Over the years phenomena driven by magnetic frustration have been studied in detail in numerous systems and naturally the geometrical frustration of triangular-lattice antiferromagnets has played a prominent role in this area of research. An extensive review of many such systems can be found in Refs. [1 and 2] where the particularities of triangular antiferromagnets with varying degrees of easy-plane or easy-axis anisotropy are described. In the majority of these systems the magnetic phase diagrams are now well understood even using conventional classical models. However, the observation of a magnetization plateau in Cs_2CuBr_4 triggered a renewed interest in the study of frustrated triangular antiferromagnets.[3,4] It is believed that this magnetization plateau is a direct manifestation of quantum fluctuations which stabilize an up-up-down (uud) state out of a multitude of degenerate configurations.[5–7]

Until recently, the only materials in this family available for study have had either distorted (isosceles) triangular lattices (such as Cs_2CuBr_4)[3,4] or effective spins larger than 1/2 (for instance $RbFe(MoO_4)_2$).[8] The subject of this work, $Ba_3CoSb_2O_9$, represents the first truly quantum (effective spin-1/2) antiferrromagnet with a perfect triangular lattice and as expected it exhibits a clear magnetization plateau in the range of 10-15 T.[9,10] Due to a strong spin-orbit coupling with a uniaxial crystal field, the ground state of Co^{2+} ions is reduced to an effective spin-1/2 moment at temperatures below ~ 250 K.[9,11] In the *ab*-plane these moments form a triangular lattice which are stacked directly on top of each other (space group $P6_3/mmc$). The dominant magnetic coupling is attributed to the nearest-neighbor exchange interaction within the plane ($J_{\parallel} = 18\ K$), while the magnetic interlayer interaction ($J_{\perp} = 0.48\ K$) is known to be much smaller as the planes are separated by double layers of nonmagnetic Sb ions.[10] $Ba_3CoSb_2O_9$ is observed to order below $T_{N1} = 3.8\ K$ and initial neutron and magnetization measurements[11,12] described this compound as a quasi-2D triangular-lattice antiferromagnet with an easy-axis anisotropy, similar to $CsNiCl_3$.[13,14] However, the absence of a second transition at zero field has raised some doubt about that designation. Based on recent ESR and NMR measurements,[10,27] there is now a clear consensus that $Ba_3CoSb_2O_9$ should rather be described as a quasi-2D triangular-lattice antiferromagnet with a weak easy-plane anisotropy.

The magnetic phase diagram for $Ba_3CoSb_2O_9$ has already been determined for $H \perp \hat{c}$ above 2 K,[12] though data at lower temperatures as well as results with the field along the *c*-axis are still scarce.[27] Thus, a detailed study of the field-induced magnetic phase diagram down to very low temperatures can potentially shed light on the effect of quantum fluctuations on the properties of frustrated triangular antiferromagnets. To that end, we have used highly sensitive sound velocity measurements down to 50 mK with a magnetic field applied parallel and perpendicular to the basal plane. The ultrasound velocity is found to be strongly coupled to the magnetic degrees of freedom, in particular the antiferromagnetic order parameters, making for a very sensitive probe of magnetic phase transitions and allowing us to determine the magnetic phase diagrams of this material with unprecedented resolution.

II. EXPERIMENT

All measurements were realized on a thin plate single crystal (0.67 mm thick) grown by the floating-zone technique.[12] Acoustic modes propagating along the *a*-

axis (within the triangular planes) were used in this investigation and were found to be well coupled to the magnetic degrees of freedom. Consequently, faces normal to the crystallographic a-direction were polished in order to mount 30 MHz $LiNbO_3$ transducers. The sample's length along the a-axis (2.57 mm) was more than sufficient to determine the velocity of the longitudinal mode and the transverse mode with polarization in the basal plane. Both sets of measurements, realized at 90 MHz using a pulsed acoustic interferometer in the transmission configuration, were used to construct the temperature-magnetic field phase diagram of $Ba_3CoSb_2O_9$ with the field parallel and normal to the c-axis. For low temperature measurements (50 mK to 2 K), an Oxford helium dilution fridge adapted for ultrasonic measurements was employed. The acoustic power as well as the repetition rate were reduced in order to avoid any potential heating at the lowest temperatures. Finally, both cryogenic systems incorporate a superconducting magnet which could produce a maximum field of 18 T.

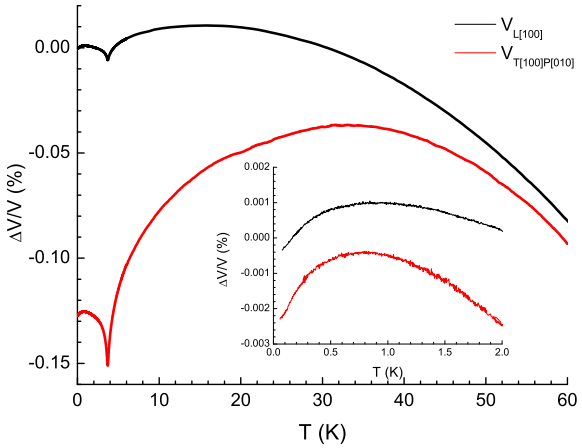

FIG. 1. Temperature dependence (in zero-field) of the relative velocity variation of the longitudinal mode $V_{L[100]}$ (black curve) and and of transverse waves polarized in the ab-plane propagating along the a-axis, $V_{T[100]P[010]}$ (red curve).

III. RESULTS

For crystals with a hexagonal symmetry,[15] the velocity of longitudinal modes propagating along the a-axis is given by $V_{L[100]} = \sqrt{C_{11}/\rho}$, while for transverse waves polarized in the basal plane $V_{T[100]P[010]} = \sqrt{C_{66}/\rho}$, where ρ is the density. Using the time of flight of acoustic pulses in the sample, we obtain that $V_{L[100]} = 5100 \pm 50$ m/s and $V_{T[100]P[010]} = 2800 \pm 30$ m/s in the paramagnetic phase ($\sim$ 100 K). As the velocity of each mode is associated with a single elastic constant, we easily obtain that $C_{11} = 17.3 \pm 0.4 \times 10^{10}$ N/m^2 and $C_{66} = 5.3 \pm 0.1 \times 10^{10}$ N/m^2.

In Fig. 1, we present the temperature dependence of the relative variation of the velocity ($\Delta V/V$) obtained for each mode. In both cases, the minimum observed at $T_{N1} = 3.81 \pm 0.01$ K agrees well with the critical temperature deduced from previous magnetic susceptibility and specific heat measurements.[11,12] Moreover, our high resolution measurements clearly establish that there is only one anomaly at zero field, contradicting previous specific heat measurements[9] which showed up to three anomalies close to T_{N1}. This observation supports an *easy-plane* anisotropy in $Ba_3CoSb_2O_9$. As shown in several other systems,[13,14,16,17] frustrated antiferromagnets with an easy-axis anisotropy would normally reveal two ordered states at zero field, one associated with a collinear order with the moments pointing along the easy-axis and an elliptical state at lower temperatures. Interestingly another effective spin-1/2 system in the same family, $Ba_3CoNb_2O_9$, was recently synthesized and proves to have a small easy-axis anisotropy with a double transition in zero field.[18,19]

The results obtained from 60 K also indicate that the velocity of both modes decreases as we approach the critical temperature T_{N1}. We attribute this softening of the elastic properties to the coupling of the lattice to extensive spin fluctuations present in the paramagnetic state, while the hardening observed at lower temperatures is evidently connected to the magnetic order which emerges below T_{N1}. The fact that the variation observed on $V_{T[100]P[010]}$ is significantly larger indicates that the coupling with the spins is enhanced for shear deformations (C_{66}). It is worth noting that the velocity of both modes decreases slightly below $T \simeq 0.8$ K (see Fig. 1 insert). This effect is discussed in more detail in section V.

In Fig. 2 we present a series of measurements obtained as a function of the magnetic field at constant temperature. Both modes have been employed in order to confirm the existence of any phase transitions with the field applied along the a-axis and the c-axis. With the field parallel to the c-axis (left end side), only one sharp anomaly is observed around $Hc_1 \simeq 12$ T on either modes. Furthermore, as shown in Fig. 3 we observe a clear field hysteresis around 12 T demonstrating that this magnetic phase transition at Hc_1 is first order. Similar measurements have been performed with the field $H \parallel \hat{a}$ (right-hand side), and in that case two minima are clearly visible in the field dependence of $V_{L[100]}$, at $Ha_1 = 9.65$ T and $Ha_2 = 14.97$ T (for $T = 0.1$ K). These two phase transitions are also confirmed by anomalies observed in $V_{T[100]P[010]}$. A small change of slope is noticeable at Ha_1 while Ha_2 is associated with a large velocity variation leading to a well defined minimum. We should emphasize that the velocity variation around Ha_2 for the transverse mode $V_{T[100]P[010]}$ is 6%, which is an order of magnitude larger than what is typically observed. In this case the magnetoelastic coupling for the transverse mode is about 60 times stronger than what is obtained for the longitudinal mode.

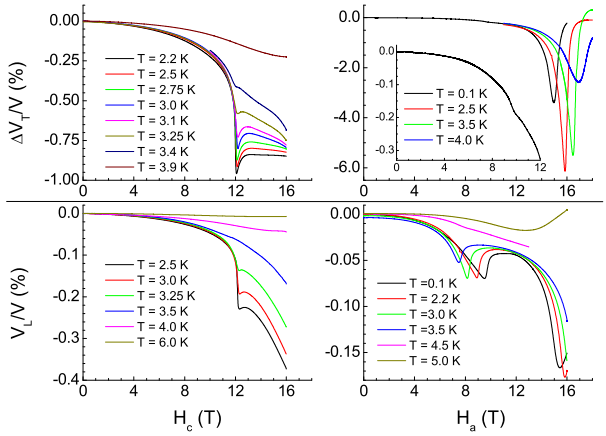

FIG. 2. Field dependence of the relative velocity variation measured at different temperatures. On the left end side we present results for $V_{T[100]P[010]}$ and $V_{L[100]}$ with $H \parallel \hat{c}$ while on the right end side we show results obtained with $H \parallel \hat{a}$.

In order to complete our investigation of the magnetic properties of $Ba_3CoSb_2O_9$, we also performed a series of measurements as a function of temperature at constant field values. For clarity, the data presented in Fig. 4 for $H \parallel \hat{a}$ have been divided into three field ranges, $H < Ha_1$, $Ha_1 < H < Ha_2$, and $H > Ha_2$. At low fields, the phase boundary corresponds to a minimum of $V_{T[100]P[010]}$, while in the intermediate range the critical temperature corresponds to the point at which the slope is at its maximum. Again, at high fields, the transverse mode velocity shows a large variation ($\Delta V/V \sim -7.4\%$ at $H = 16$ T) with the transition associated with a minimum on each curve. With the field applied along the

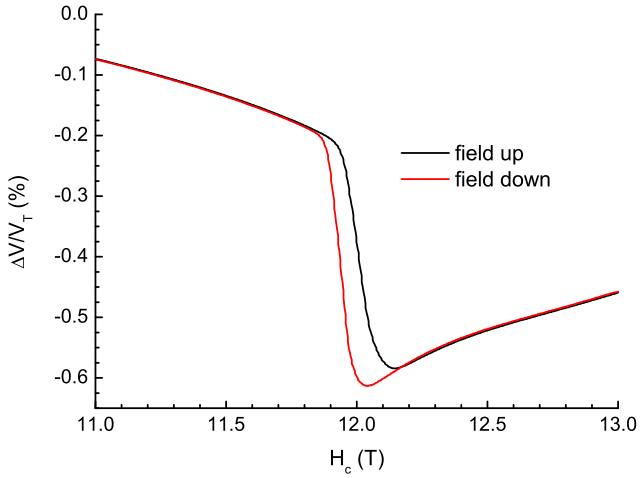

FIG. 3. Relative velocity variation of the transverse mode showing the field hysteresis for the first order phase transition observed at 12 T with $H \parallel \hat{c}$

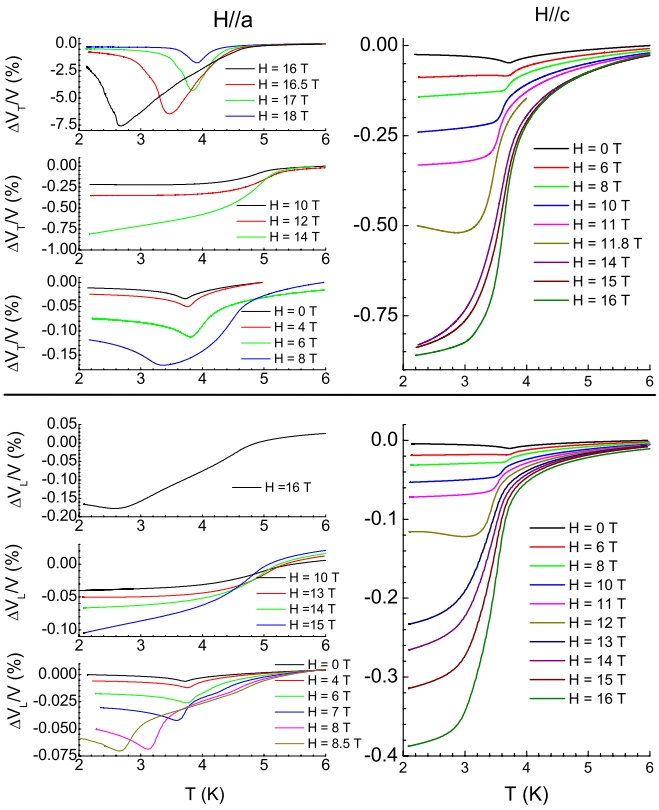

FIG. 4. Temperature dependence of the relative velocity variation measured at different fields. On the left end side we present results for $V_{T[100]P[010]}$ and $V_{L[100]}$ with $H \parallel \hat{c}$ while on the right end side we show results obtained with $H \parallel \hat{c}$.

c-axis both modes show the same type of evolution. As the field increases, the minimum in the velocity is gradually replaced by a region where the slope is maximal. We also notice that the variation above the critical temperature, which we associate with magnetoelastic effects, increases significantly as the field is increased ($\sim -0.25\%$ just above 4 K on $V_{T[100]P[010]}$).

IV. MAGNETIC PHASE DIAGRAM OF $BA_3COSB_2O_9$

These sets of velocity measurements as a function of temperature and field have been used to construct the magnetic phase diagram of $Ba_3CoSb_2O_9$ for $H \parallel \hat{a}$ and $H \parallel \hat{c}$. The phase boundaries presented in Fig. 5 have been obtained using anomalies observed on $V_{T[100]P[010]}$ and $V_{L[100]}$ where the temperature and the field have been cycled in order to identify first order transitions. Our phase diagram for $H \parallel \hat{a}$ agrees well with the phase diagram previously obtained from magnetization and specific-heat studies described in Ref. 12 (note that the phase diagram labeled as $H \parallel \hat{c}$ in Ref. 12 is in fact corresponds to $H \parallel ab$-plane). At low temperatures a sequence of four different magnetic orders, all with three

sub-lattices, are assumed as the field is increased. At zero field the ground state corresponds to the 120° order commonly observed in easy-plane antiferromagnetic systems with a triangular lattice[1,13,21,22]. So far several different theoretical approaches have been proposed in order to identify field induced phases of classical or spin-1/2 triangular-lattice antiferromagnets.[23–26] In general these approaches all identify the same sequence of phases. With the magnetic field applied in the basal plane, the 120° spin configuration is distorted and gives rise to a configuration labeled as the coplanar Y-state. This is followed by a colinear up-up-down (uud) state leading to a magnetization plateau ($M = M_s/3$) at $H_{a1} = 9.7\ T$, and finally a coplanar V-state above $H_{a2} = 15.0$ T. All of these predicted states are consistent with NMR spectra obtained by Koutroulakis *et al.*[27]

Recent NMR relaxation[27] and magnetization[10] measurements also find clear evidence of an additional phase transition around $H_{a3} = 22\ T$, which is not accounted for in isotropic triangular lattice models. Koutroulakis *et al.*[27] have proposed that this is a transition between two different kinds of V-like orders, the primary difference being the relationship between spins in adjacent *ab*-planes, although the NMR spectra cannot unambiguously differentiate these two states.[27] It is possible that this additional phase could be the result of a distortion associated with magnetostriction effects which break the hexagonal symmetry whenever the field is applied in the basal-plane.[25] However, for the time being there is no experimental evidence that these field induced deformations are sufficiently large to play a significant role in the magnetic properties of $Ba_3CoSb_2O_9$. Our work has demonstrated that the spin-lattice coupling is indeed very strong, with changes in sound velocity as large as 7%, and therefore has laid the groundwork for a more in-depth study of the effects of magnetostriction on the phase diagram of this compound.

Here we present the first detailed phase diagram of this material for $H \parallel \hat{c}$. Previous work showed the existence of several phases for this field direction but only obtained a rough schematic phase diagram based on several data points.[27] As shown in Fig. 5, with the field applied normal to the basal plane (H_c) only one phase transition is observed (in our range of magnetic field) at $H_{c1} = 12.0\ T$. Contrary to all other transitions observed for this compound, our sound velocity measurements show clear evidence of a field hysteresis at H_{c1} (Fig. 3), demonstrating that the character of this particular transition is first order. This hysteresis is clearly observed for both modes and does not depend on the magnetic field sweep rate. We believe that this observation is also consistent with susceptibility measurements[10] which show a pronounced peak at H_{c1}. Moreover, considering that magnetization measurements[10] show no clear magnetization plateau above that critical field, we must assume that the magnetic anisotropy plays a significant role in selecting one of several possible magnetic states for the field along the *c*-axis.

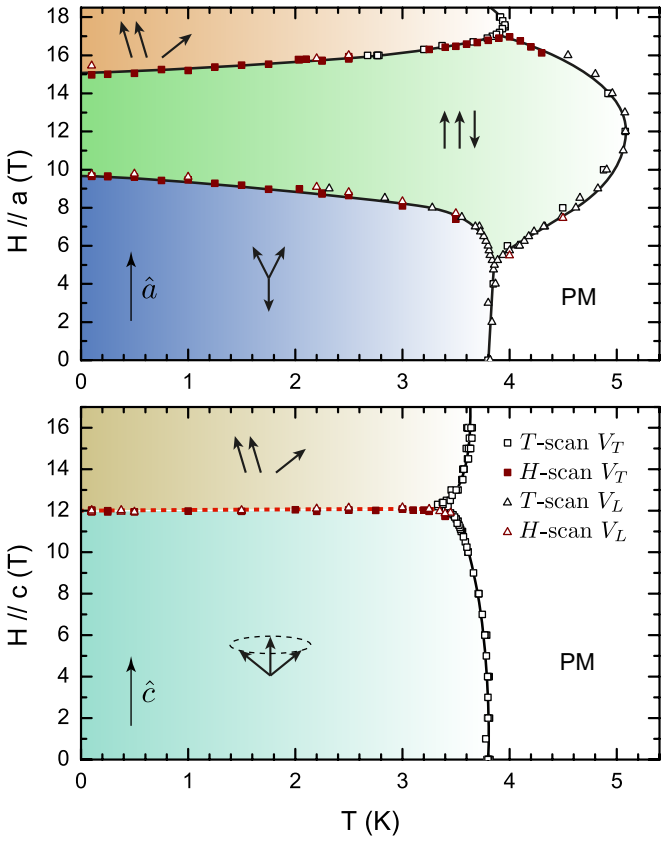

FIG. 5. Experimental phase diagrams of $Ba_3CoSb_2O_9$ for $H \parallel \hat{a}$ and $H \parallel \hat{c}$ obtained from sound velocity measurements as a function of temperature (black points) and field (red points). Solid black lines indicate continuous phase transitions whereas the dotted red line (for $H \parallel \hat{c}$) indicates a line of first-order phase transitions.

One simple approach to determining the actual magnetic configurations is to consider a Landau model for a Heisenberg antiferromagnet system with hexagonal symmetry and an easy-plane anisotropy. This type of model has been studied in detail and, as shown in Ref. 13, one possible scenario involves an umbrella-type configuration (120° spin structure in the basal-plane with a uniform component along the field direction) that suddenly changes into a coplanar Y-type order with all spins lying in a plane including the *c*-axis. In that case, the basal-plane components associated with the easy-plane anisotropy flip into a new plane orientation giving rise to a first order spin-flop transition (see Fig. 7a of Ref. 13). As the field is increased further, a continuous phase transition into a collinear order with all spins pointing along the *c*-axis is also predicted. So far no such anomaly has been observed on high field magnetization measurements.[10] Another scenario is that for spin-1/2 frustrated systems, such as $Ba_3CoSb_2O_9$, specific spin structures might emerge from thermal or quantum fluctuations as discussed in Nikuni *et al.*[28] Even in that case, a first order spin-flop transition from the umbrella-type

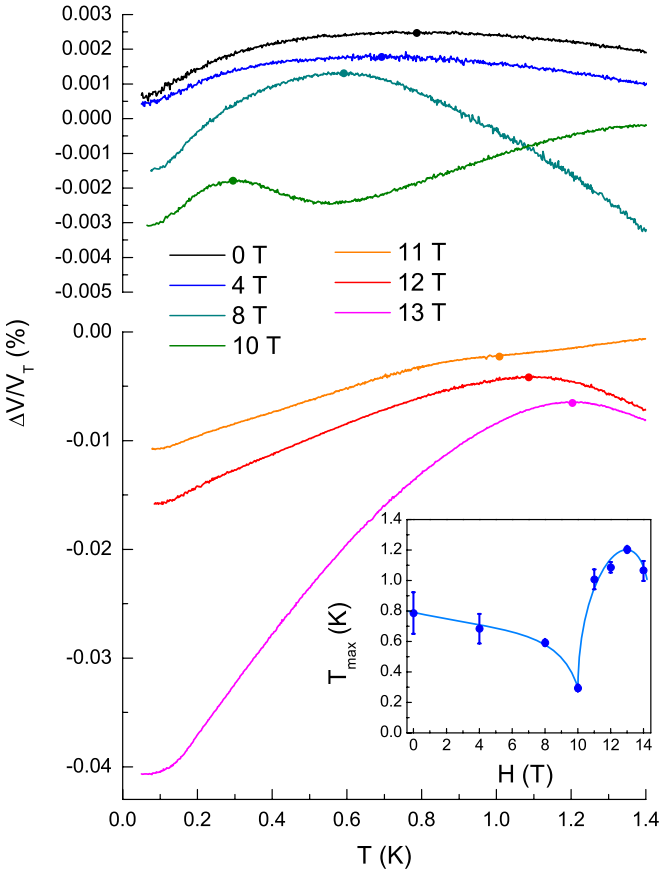

FIG. 6. Low temperature sound velocity measurements showing an unusual softening of the lattice at temperatures below 1 K. The round data points indicate the maximum (or inflection point for $H = 11$ T), $T_{\max}$, that we identify as the onset of the low-temperature lattice softening. The inset shows $T_{\max}$ as a function of $H \parallel \hat{a}$. $T_{\max}$ exhibits a clear cusp at around 10 T, which coincides with the field-induced phase transition from Y-type to *uud* order.

configuration to a Y-type or V-type coplanar configuration is expected. Given that the magnetization immediately above the spin-flop transition is greater than 1/3 of the total magnetization,[10] which is incompatible with a Y-type configuration, this state is more likely a V-type order.

V. RESIDUAL SPIN FLUCTUATIONS

As shown in the inset of Fig. 1, the sound velocity (in both modes) is found to decrease below $T \simeq 0.8$ K in zero field. The sound velocity is normally expected to be temperature independent in this range since the phonon population vanishes at very low temperatures.[20] Thus this change is likely magnetic in origin, an assumption that is supported by a strong magnetic-field dependence as illustrated in Fig. 6. It is highly unlikely that this softening of the lattice could result from a reduction in the order parameter as the change is not sharp enough to signify an additional phase transition. Therefore, we attribute this reduction in velocity to a coupling of the lattice to residual spin fluctuations. As the temperature is lowered these fluctuations have increased spectral weight at low frequencies (and are perhaps beginning to freeze) and this leads to a softening of the lattice at the measurement frequency (30 MHz). Since we never observe the lattice to stiffen again on decreasing the temperature, these fluctuations must persist to as low as 50 mK, almost two orders of magnitude lower than T_C. Such persistent spin dynamics (PSDs) are a common feature of frustrated magnets as seen by muon spin rotation (μSR), neutron spin echo and Mössbauer spectroscopy measurements.[29–32] To our knowledge, this is the first observation of such residual fluctuations with sound velocity measurements. Zhou *et al.*[12] observed a continuum of spin excitations, possibly spinons, in the ordered phase of this material with inelastic neutron scattering, again suggesting that the ground state is not entirely conventional.

In the inset of Fig. 6 we present the effect of magnetic field, $H \parallel \hat{a}$, on $T_{\max}$, the temperature at which the velocity passes through a maximum and the low-temperature softening begins. Notably in the vicinity of the phase transition (from Y-type to *uud* order) at 10 T, the lattice softening is pushed to much lower temperatures. It is perhaps unsurprising to observe that in the vicinity of a quantum phase transition spin fluctuations remain fast and do not couple to our measurement until very low temperatures. We did not observe this low-temperature softening at 16 T, suggesting that these residual spin fluctuations are absent in the V-type phase.

VI. SUMMARY AND CONCLUSIONS

Using anomalies observed in the field and temperature dependence of the velocity of longitudinal and transverse sound waves we have obtained a high-precision magnetic phase diagram of $Ba_3CoSb_2O_9$ for $H \parallel \hat{a}$ and $H \parallel \hat{c}$. As discussed, the results obtained in this work for $H \parallel \hat{a}$ are consistent with predictions made using 2D isotropic Heisenberg models and with previous studies. Furthermore, our data obtained for $H \parallel \hat{c}$ confirm that the easy-plane anisotropy cannot be ignored in the description of this system.[28] Nonetheless, the anisotropy alone cannot account for the additional state observed for $H \parallel \hat{a}$. It seems that the interlayer coupling ($J_\perp$)[27] and possible distortions of the triangular lattice (J'/J) at high fields might be necessary to fully account for the magnetic properties of $Ba_3CoSb_2O_9$.[24,25] This work highlights the fact that certain lattice modes are highly coupled to the magnetic degrees of freedom of this material. Thus future experimental works that explicitly measure contributions of magnetostriction to this physics of this compound might be the key to determining the relevance of distorted triangular lattice models. Finally we have also discovered a surprising lattice softening that occurs at $T \simeq T_C/5$ or lower which we have attributed to residual

spin fluctuations that persist to the lowest temperatures measured.

VII. ACKNOWLEDGMENTS

The authors wishes to thank Dr. M. L. Plumer for very valuable discussions. We also acknowledge technical support from M. Castonguay. This work was supported by the Natural Sciences and Engineering Research Council of Canada (NSERC) and the Fonds de recherche du Québec – Nature et technologies (FRQNT). Z.L.D. and H.D.Z. acknowledge the support of NSF-DMR- 1350002.

* Department of Physics and Physical Oceanography, Memorial University, St. John's, Newfoundland, Canada, A1B 3X7

[1] M. F. Collins and O. A. Petrenko, Can. J. Phys. **75**, 605 (1997).
[2] H. T. Diep, Frustrated spin systems (World Scientific Publishing Co. Pte. Ltd., 2013).
[3] T. Ono, H. Tanaka, H. Aruga Katori, F. Ishikawa, H. Mitamura, and T. Goto, Phys. Rev. B **67**, 104431 (2003).
[4] N. A. Fortune, S. T. Hannahs, Y. Yoshida, T. E. Sherline, T. Ono, H. Tanaka, and Y. Takano, Phys. Rev. Lett. **102**, 257201 (2009).
[5] A. V. Chubukov and D. I. Golosov, J. Phys.: Condens. Matter **3**, 69 (1991).
[6] J. Alicea, A. V. Chubukov, and O. A. Starykh, Phys. Rev. Lett. **102**, 137201 (2009).
[7] C. Lacroix, P. Mendels, and F. Mila, Introduction to Frustrated Magnetism (2011).
[8] J. S. White, C. Niedermayer, G. Gasparovic, C. Broholm, J. M. S. Park, A. Y. Shapiro, L. A. Demianets, and M. Kenzelmann, Phys. Rev. B **88**, 060409 (2013).
[9] Y. Shirata, H. Tanaka, A. Matsuo, and K. Kindo, Phys. Rev. Lett. **108**, 057205 (2012).
[10] T. Susuki, N. Kurita, T. Tanaka, H. Nojiri, A. Matsuo, K. Kindo, and H. Tanaka, Phys. Rev. Lett. **110**, 267201 (2013).
[11] Y. Doi, Y. Hinatsu, and K. Ohoyama, Journal of Physics: Condensed Matter **16**, 8923 (2004).
[12] H. D. Zhou, C. Xu, A. M. Hallas, H. J. Silverstein, C. R. Wiebe, I. Umegaki, J. Q. Yan, T. P. Murphy, J.-H. Park, Y. Qiu, et al., Phys. Rev. Lett. **109**, 267206 (2012).
[13] M. L. Plumer, A. Caillé, and K. Hood, Phys. Rev. B **39**, 4489 (1989).
[14] G. Quirion, X. Han, and M. L. Plumer, Phys. Rev. B **84**, 014408 (2011).
[15] E. Dieulesaint and D. Royer, Elastic Waves in Solids (John Wiley and Sons Ltd., 1980).
[16] G. Quirion and M. L. Plumer, Phys. Rev. B **87**, 174428 (2013).
[17] R. Villarreal, G. Quirion, M. L. Plumer, M. Poirier, T. Usui, and T. Kimura, Phys. Rev. Lett. **109**, 167206 (2012).
[18] K. Yokota, N. Kurita, and H. Tanaka, Phys. Rev. B **90**, 014403 (2014).
[19] M. Lee, J. Hwang, E. S. Choi, J. Ma, C. R. Dela Cruz, M. Zhu, X. Ke, Z. L. Dun, and H. D. Zhou, Phys. Rev. B **89**, 104420 (2014).
[20] Y. P. Varshni, Phys. Rev. B **2**, 3952 (1970).
[21] M. L. Plumer and A. Caillé, Phys. Rev. B **42**, 10388 (1990).
[22] M. L. Plumer and A. Caillé, J. Appl. Phys. **69**, 6161 (1991).
[23] M. V. Gvozdikova, P.-E. Melchy, and M. E. Zhitomirsky, Journal of Physics: Condensed Matter **23**, 164209 (2011).
[24] T. Coletta, M. E. Zhitomirsky, and F. Mila, Phys. Rev. B **87**, 060407 (2013).
[25] R. Chen, H. Ju, H.-C. Jiang, O. A. Starykh, and L. Balents, Phys. Rev. B **87**, 165123 (2013).
[26] D. Yamamoto, G. Marmorini, and I. Danshita, Phys. Rev. Lett. **114**, 027201 (2015).
[27] G. Koutroulakis, T. Zhou, Y. Kamiya, J. D. Thompson, H. D. Zhou, C. D. Batista, and S. E. Brown, Phys. Rev. B **91**, 024410 (2015).
[28] T. Nikuni and H. Shiba, J. Phys. Soc. Japan **62**, 3268 (1993).
[29] Y. Chapuis *et al.*, Physica B **404**, 686 (2009).
[30] S. J. Blundell, Phys. Rev. Lett. **108**, 147601 (2012).
[31] P. Dalmas de Réotier *et al.*, Phys. Rev. B **85**, 140407(R) (2012).
[32] J. A. Quilliam *et al.*, Phys. Rev. Lett. **109**, 117203 (2012).